PSK modulation in camera based VLC for receiving from distributed transmitters

Wataru Kihara*, Tomohiro Yendo* Yoshifumi Shiraki†, Takashi G. Sato†, Takehiro Moriya†
*Department of Electrical, Electronics and Information Engineering
Nagaoka University of Technology, 1603-1, Kamitomioka-machi, Nagaoka, Niigata, 940-2188, JAPAN
Email: s143125@stn.nagaokaut.ac.jp
† NTT Communication Science Laboratories, Nippon Telegraph and Telephone Corporation
3-1 Wakamiya, Morinosato, Atsugi, Kanagawa, 243-0198, JAPAN

***Abstract*—Visible light communication (VLC) is an optical wireless communication technology that operates in the visible spectrum. Image-sensor based VLC, also as known as optical camera communication is a powerful method for receiving data from distributed transmitters. This paper discusses methods that modulate the data from the distributed transmitters, and proposes a communication method using two image-sensors. The proposed method uniquely estimate the phase difference between the camera framing and LED blinking from two pixel values obtained by two cameras with different exposure timings, and communicates by phase shift keying. The principle of the proposed method is confirmed in experiments.**

I. Introduction

Visible light communication (VLC) is an optical wireless communication technology in which light-emitting diodes (LEDs) serve as both light providers data broadcasters[1][2]. LEDs are energy-efficient and widely used in general lighting applications. Owing to the high response speed of LEDs, VLC can send data by light blinks that flicker below the detectable limit of human eyes. As VLC communication is not restricted by a bandwidth of radio waves, it proceeds in environments where conventional wireless communication such as Wi-Fi cannot be operated stably. This is a major advantage of VLC.

Fig. 1 shows the remote sensing application assumed in this study. The data from the distributed transmitters are received by a powerful method called image-sensor based VLC also termed optical camera communication (OCC). To simplify the transmitter, we assume that multiple transmitters independently operate with their own clock. Therefore, the method must implement asynchronous communication. Moreover, because the symbol rate in image-sensor based VLC is limited by the camera frame rate, multi-level modulation that improves the information transfer rate per symbol (and hence the communication speed,) is desired. The proposed image-sensor based VLC designed to accomplish these tasks.

This paper discusses modulation methods for the image-sensor based VLC, and propose a communication method using Phase Shift Keying (PSK). The proposed method uniquely estimates the phase difference between the exposure timing and LED blinks from two pixel values obtained by two cameras with different exposure timings. Moreover, the proposed method can communicate when the camera framing and transmitter are asynchronous. The principle of the proposed method by experiments is confirmed in experiments.

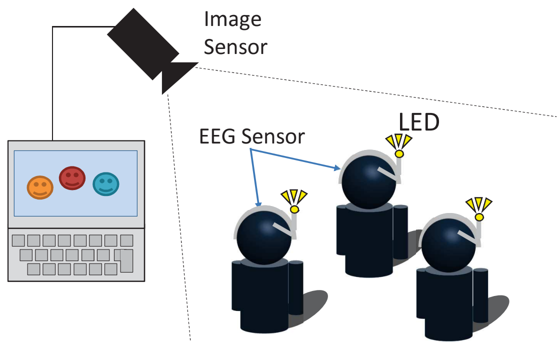

Fig. 1. Assumed application in this study. In this scene, brain wave signals of multiple people are simultaneously measured by the image-sensor based VLC system.

II. Related Research

In previous studies, data from multiple transmitters were received by image-sensor based VLC. Pablo et al. developed an optical wireless audio system that exploits the parallel transmission feature of arranged LEDs and a high-speed camera[3]. This system observes sound fields by optical wireless acoustic sensors (OWAS). Each OWAS comprises a 4×4 LED matrix, a microphone, and a IR sensor. The sound data are transmitted by visible light on off keying (OOK), and the transmission data are demodulated by high-speed parallel processing of the image observed by a high-speed camera using general purpose graphic processing unit (GPGPU). To synchronize the multiple OWASs with the camera framing, the same master-clock signal is broadcasted to the OWASs via infra-red rays. This method achieves directional sound collection in real-time.

Elsewhere, Sato et al. incorporated VLC in multi-biosignal sensing[4]. They proposed the ET encoding method for capturing the heart rates of multiple people by image-sensor based VLC with a low frame rate. Multi-biosignal sensing techniques included recording of electroencephalogram (EEG) data are expected to be applied in medical monitoring and remote sports coaching system. Multi-biosignal system in Fig.1 measures the EEG signals of multiple users by VLC. In

Published by Visible Light Communications Associated at "2nd International Conference and Exhibition on Visible Light Communications 2018" on March 16, 2018 in Yokohama, Japan.

the present paper, this system is assumed as an application of our proposed method. To cope with the subject's movements, a simple transmitter is desired.

To decide the optimal method for the assumed application, we investigated image-sensor based VLC in various scenarios. We first considered the VLC with a high-speed camera used in intelligent transport systems, which have received considerable attention in recent years[5]-[7]. In such case, OOK is a widely-used modulation method. Owing to the high camera frame rate, the LEDs send data at blinking speeds that are undetectable to the human eyes. In image-sensor based VLC, the camera frame rate limits communication. Therefore, a high camera frame rate realizes a high-speed communication.

Another method exploits the rolling shutter feature of a CMOS sensor[8]. The transmitter in this method is a plane light source or an indirect light, which is captured by the camera within a large area of the sensor. In a CMOS sensor, the pixels are exposed row by row. The rolling shutter divides time as the line scan proceeds, so quick changes in the light manifest captured as light and dark patterns on the image. High-speed communication is realized by using this light and dark pattern. Oshima et al. achieved high-speed communication using a normal-speed image-sensor[9]. However, because our research assumes communication with distributed LEDs, our transmitters are point-light sources and the rolling shutter method is unsuitable.

Luo et. al proposed the UPSOOK method[10], which supports non-flickering VLC using a normal-speed camera and point-light sources. In their method, the exposure time of the camera is set significantly shorter than the LED blinking period. The camera receives data by estimating three type of light symbols created by changing the frequency and phase of the LED blinking. This method can also communicate when the camera framing and LED blinks are asynchronous. However, the type of symbols is three in their method and multi-valuing is difficult. In addition, the very short exposure time yields a very dark image.

Finally, Shimada et al. estimated the amplitude and phase difference from multiple frame images using a single camera and a single LED[11]. The LED is modulated with a frequency of one-third the frame rate and the camera captures a LED three frames for one symbol. The modulated light is restored as a virtual sine wave from the three pixel values and the phase and amplitude can be uniquely estimated. This method achieves multi-level communication by quadrature amplitude modulation. However, in the experiments, the receiver and transmitter were operated by the same signal generator, and the camera framing and modulation timing are synchronized.

Methods that would resolve the problems in the above image-sensor based VLC methods have not been proposed. Therefore, a new communication method is required.

III. Consideration of modulation method

We assume that data are received from asynchronous and distributed transmitters. To improve the communication speed, we require multi-level modulation which transmit more information per symbol. We also desire a simple transmitter for the assumed application. Before devising a method that resolves these problems, we discuss various modulation and communication method.

As mentioned above, OOK is one of the most widely used modulation method in VLC. However, amplitude shift keying (of which OOK is the simplest type) is unsuitable for our current application for reasons. First, multi-level modulation requires multi-level control of the current which complicates the drive circuit. Second, as the symbol rate is generally set lower than the frame rate, human eyes will detect flicker if a normal-speed camera is used. Methods that resolve these problem are imperative.

Phase shift keying (PSK) requires no current control in multi-level modulation, so is expected to simplify the transmitter constructs. Moreover, the flicker problem is easily solved by increasing the blinking frequency. Therefore, we apply PSK as the modulation method in our research.

We now outline communication by PSK. When with a short exposure time drives the LED blinking, the pixel value varies by the relationship between the camera framing and LED blinking. Therefore, the phase difference can be estimated from the pixel values. However, as one pixel value corresponds to two phases, the phase estimation from a single pixel value is ambiguous.

This ambiguity can be removed by using the two-LED transmitter[12]. The two-LED whose blinking phase are different 90° each other, and the phase difference between the camera framing and LED blinking can be uniquely estimated from the pixel values of the two-LED. However, we assume the use of a large number of transmitter in this study. In this case, the simple transmitter is preferred for easier identification of transmitter in the receiver side.

The proposed method uses two cameras with different exposure timings. In this setup, the phase difference between the transmitter and receiver can be estimated from two pixel values. Whereas Shimada et al.'s single-camera/single-LED method requires three frames for estimating the phase difference[11], our two-cameras method estimates the phase from one frame of both cameras.

IV. Method

A. Phase-estimation method

In our phase-estimation method, the frequency of the LED blinking is set to integer multiple of the frame rate of the camera and the duty rate is set to 50%. When the exposure time is sufficiently longer than the LED blinking period, the pixel value of the captured image remains almost constant, irrespective of the relationship between the exposure timing and LED blinking. When the exposure time is shorter than the LED blinking period, the pixel value varies by the phase difference between the exposure timing and the LED blinking. Fig. 2 shows the response of the pixel value to a change in the relationship between exposure timing and blinking.

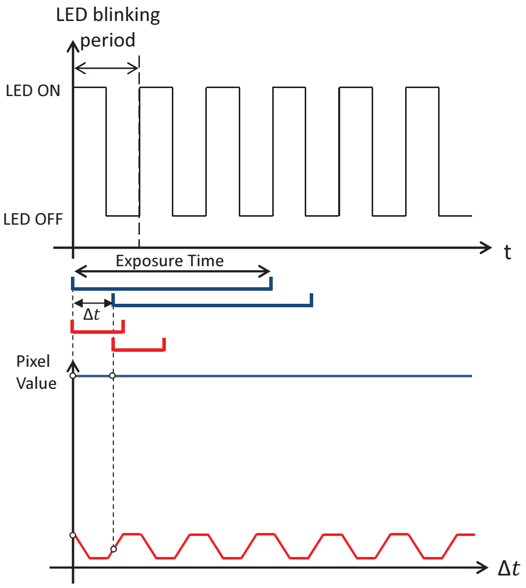

Fig. 2. Response of the pixel value to a change in the relationship between exposure timing and blinking. The upper figure shows the LED blinking waveform when duty is 50 %, and the bottom figure shows the change of pixel value due to the relationship between the exposure timing and blinking. The part shown in blue is case of the exposure time is long. In contrast, the part shown in red is case of the exposure time is short.

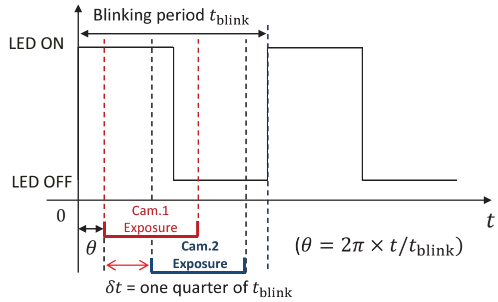

(a) LED blinking waveform

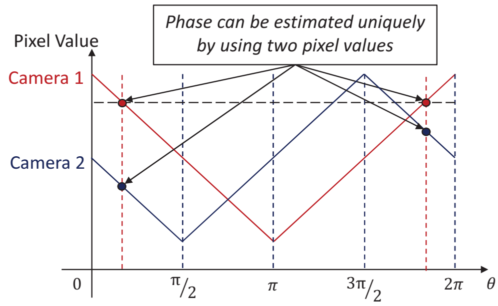

(b) Pixel values change according to the change of relationship between camera framing and LED blinking

Fig. 3. Relationship between the pixel values and the phase difference

When the exposure time t_{exp} is one-half of the LED blinking period t_{blink}, the pixel value linearly varies by the phase difference between the exposure timing and LED blinking θ, as shown in Fig. 3(b). Note that t_{exp} and t_{blink} are not directly related to the symbol rate.

To resolve the above mentioned phase ambiguity in each pixel value, we employ two cameras with different exposure timings. The timings are separated by one-quarter of the LED blinking period t_{blink} as shown in Fig. 3(a). The two pixel values obtained by the two cameras, provide a unique phase estimation (see Fig. 3(b)).

The pixel values obtained by the two cameras (PV_1, PV_2) are given by :

$$(PV_1, PV_2) = \begin{cases} (1-\frac{\theta}{\pi}, \frac{1}{2}-\frac{\theta}{\pi}) & (0 \le \theta < \frac{\pi}{2}) \\ (1-\frac{\theta}{\pi}, \frac{\theta}{\pi}-\frac{1}{2}) & (\frac{\pi}{2} \le \theta < \pi) \\ (\frac{\theta}{\pi}-1, \frac{\theta}{\pi}-\frac{1}{2}) & (\pi \le \theta < \frac{3\pi}{2}) \\ (\frac{\theta}{\pi}-1, \frac{5}{2}-\frac{\theta}{\pi}) & (\frac{3\pi}{2} \le \theta < 2\pi) \end{cases} \quad (1)$$

where PV_1 and PV_2 are normalized into 0 to 1. Fig. 4 shows the theoretical trajectory given by Eq. (1).

The phase difference θ are given by two pixel values as :

$$\theta = \begin{cases} \pi(1-PV_1) & (PV_1 > 0.5, PV_2 \le 0.5) \\ \pi(\frac{1}{2}+PV_2) & (PV_1 \le 0.5, PV_2 \le 0.5) \\ \pi(1+PV_1) & (PV_1 \le 0.5, PV_2 > 0.5) \\ \pi(\frac{5}{2}-PV_2) & (PV_1 > 0.5, PV_2 > 0.5) \end{cases} \quad (2)$$

B. Estimation method considering the error of pixel value

Owing to noise in the measurement system, the pixel values measured by the cameras deviate from the theoretical trajectory on the $PV_1 - PV_2$ plane. To diminish this error, we devised the method outlined in Fig. 5. In this method, we set a line from the center to the observed point and estimate the phase from the intersection of the set line with the theoretical trajectory.

C. Error caused by asynchronous communication and its solution

This method sets the symbol rate is set slightly smaller than the camera frame to avoid the use of inappropriate frames (hereafter, called ”Error-Frame”) in the decoding.

The error caused by asynchronous communication is explained as follows. As the clocks of the camera framing and

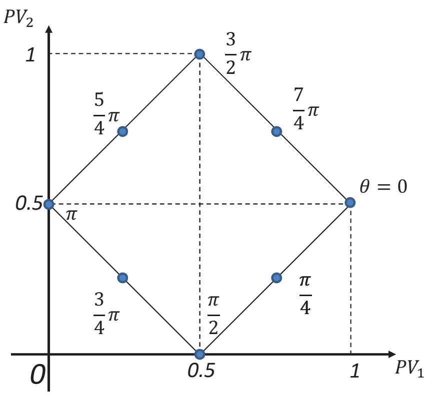

Fig. 4. Theoretical trajectory of the pixel values PV_1 and PV_2 in the PV_1-PV_2 plane. The pixel values move on this trajectory according to changing of phase difference.

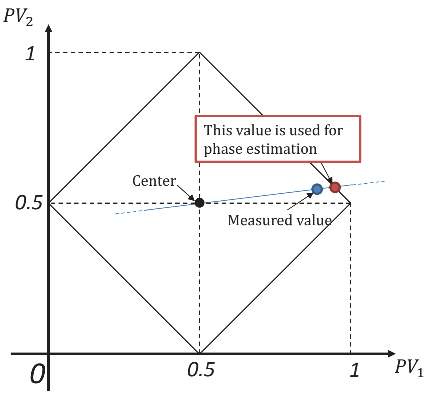

Fig. 5. Outline of our proposed method for improving the phase-estimation accuracy

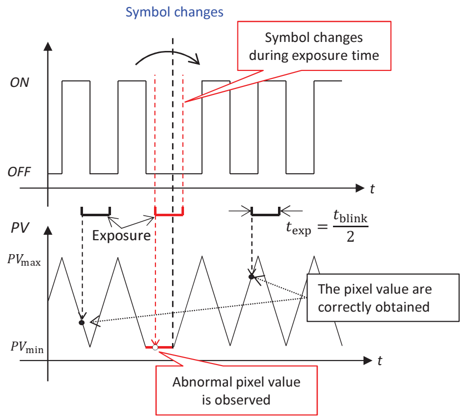

Fig. 6. The error due to changing symbol during exposure time

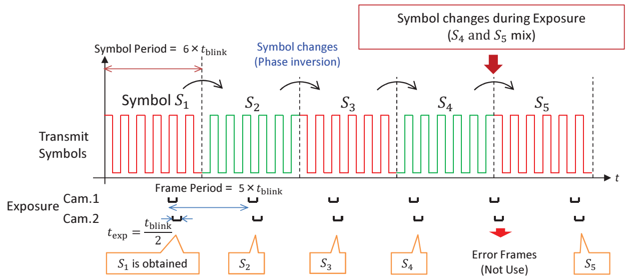

Fig. 7. Outline figure of the error solving method

LED blinking are not synchronized, the transmitted symbols might alter during the camera exposure time. If the symbol changes during the exposure time, the phase cannot be estimated because the pixel values are influenced by both symbols either before and after changing (red sections in Fig. 6).

Fig. 7 outlines our solution to this problem. The frequency of the LED blinking is set to integer n multiple of the camera frame rate, and the symbol period is set to $(n+1)t_{\mathrm{blink}}$. Two symbols are mixed in the Error-Frame which is observed once every $(n+1)$ frames, both symbols can be obtained either before or after the frame (see Fig. 7). Therefore errors can be avoided by detecting the Error-Frame once at the beginning of the packet and excluding that frame from the packet decoding. Here, the Error-Frame is detected by adding the sequence be composed of symbols whose phase shifted alternately to the beginning of the packet.

In real situation, the frequency difference between the transmitter and receiver gradually changes the relationship between the camera framing and LED blinking. However, we can assume that during a packet transmission, this drift is negligibly small.

V. Experiments

A. Conditions of experiments

1) Packet composition: Fig. 8 shows the LED blinking patterns of a packet (comprising the header and the data part) during the experiment. The preamble in the header part identifies the beginning of the packet and five symbols are used for detecting the Error-Frame. During the preamble, the LED is not blinked and the current is controlled so that the intermediate pixel values are captured by both cameras. Thereby, the cameras capture the unique pixel values and uses them to detect the communication start. The length of preamble is set to $10 \times t_{\mathrm{blink}}$. The Error-Frames are detected using the sequence be composed of five symbols whose phase shifted alternately. The symbol period is $6 \times t_{\mathrm{blink}}$ from this part until the end of the packet. The reference phase of the PSK also detects in this part. In the data part, the number of transmit symbols is set to integer multiple of the number of blinks per frame period, under the constraint of our error solving method. In the experiments, the number of data symbols number was set to 50.

2) Devices and Settings: Fig. 9 is a photograph of the experimental setup.

At the receiver side, we installed two Point Gray research's Flea 3 (FL3-U3-13E4M-C) cameras. The camera resolution was (1280 $\times$ 1024) pixels. The two cameras were controlled by different PCs and the image were captured by FlyCap 2

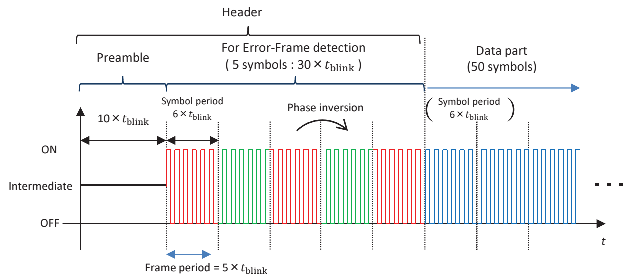

Fig. 8. LED blinking patterns of the packet

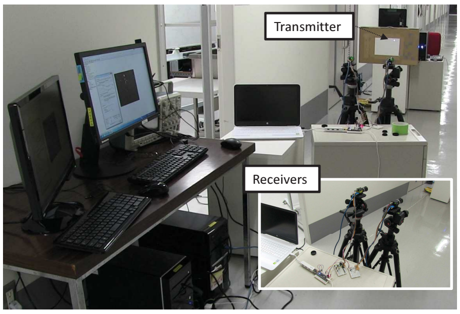

Fig. 9. Experiment view

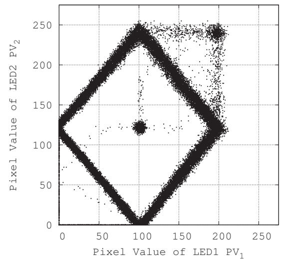

(a) BPSK

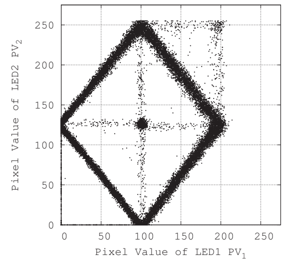

(b) QPSK

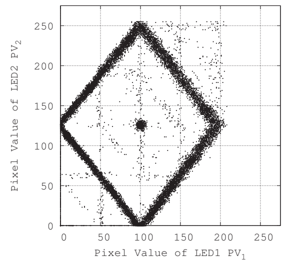

(c) 8PSK

Fig. 10. Measured pixel values

software. The framings of the both cameras were controlled by our own trigger signal generation circuit, providing a frame rate of 60 fps. The camera framings differed by 0.833 ms. The exposure time and gain of the cameras were set to 1.665 ms and 0 dB, respectively. We used two SPACECOM's JHF8M-MP camera lenses, each with a focal length of 8 mm. The cameras were separated by approximately 20cm.

At the transmitter side, we installed a Cree's Full-color LED (CLP6C-FPB) controlled by a TLC5922 LED driver (Texas Instruments). The LED blinking frequency of LED was set to 300 Hz. The symbol rate are calculated as following: the frame rate times the number of data symbol per packet over the number of captured frames per packet. In this experiment, the symbol rate was calculated as: $60 \times 50/68 = 44.1sps$.

Demodulation was performed on a different PC using images from both cameras captured in advance. The transmitter was set approximately 10 m from the receiver in an indoor environment.

B. Communication experiment

In the experiment, we measured bit error rate (BER) during the transmission of 30,000 bits. The transmitted data were randomly selected binary bits. The modulation methods were binary PSK (BPSK), quadrature PSK (QPSK) and eight-PSK (8PSK).

Fig. 10 shows the measured pixel values plotted on the $PV_1 - PV_2$ plane.

Many of the measured values approached the theoretical trajectory shown in Fig. 4. The intermediate values were measured in the preamble, and the deviations from the theoretical trajectory were considered to arise when the symbol shifted during the exposure time. Table I shows the BERs measured by each modulation method. Under 8PSK modulation, the BER was of order 10^{-3}.

TABLE I
MEASURED BER DURING 30,000-BITS TRANSMISSION MODULATED BY DIFFERENT METHODS

Modulation Method	BER
BPSK	4.33×10^{-4}
QPSK	6.67×10^{-4}
8PSK	3.13×10^{-3}

VI. Discussion

This section discuss the experimental results and proposes ideas for future work.

A. Measured pixel values

Fig. 10 shows the pixel values measured in the experiments. The intermediate values were measured in the preamble, and the deviations from the theoretical trajectory probably arise from symbol shifts during the exposure time. Because the modulation method alters the number of shifting patterns of the phases, it also affects the pixel values observed in the Error-Frame (Fig. 10).

B. Causes of error

The measured BER are listed in Table I. Errors are caused by failures in the Error-Frame detection most likely arising from vulnerability in the Error-Frame detection protocol. As described in Section IV-C, we solved the error caused by asynchronous communication by a specially designed method. The Error-Frame detection method uses the error of estimated phase in the Error-Frame and it is performed by threshold detection. We experimentally determined the threshold to obtain the best demodulation result. However, the Error-Frame cannot be completely detected. Therefore, the Error-Frame detection algorithm is considered that is incomplete. To resolve this problem, we will consider direct comparison of the pixel values in future work. When the symbol changes during the exposure time, the pixel values in the Error-Frame depart from the theoretical trajectory (Fig. 10). Therefore, we consider that the Error-Frame can be detected by the Euclidean distance between the measured value and theoretical trajectory on the $PV_1 - PV_2$ plane. Moreover, this method detects the error frame from the pixel values observed in the data symbols, the accuracy of Error-Frame detection expected to be improved. Optimizing the protocol will be attempted in future work.

C. Applications of the Proposed Method

Our proposed VLC method uses two image-sensors. The method assumes communication with distributed transmitters, and resolves the asynchronous communication problem. Moreover, we confirmed that the proposed method can communicate by multi-level PSK.

Communication with distributed transmitters requires additional tasks that were not considered here. Firstly, as the LED transmitters are spatially dispersed the LEDs are placed at different distances from the cameras. Consequently, the magnitudes of the obtained pixel values and their sizes in the image differ. When the width of a pixel value changes, an error occurs in the phase estimation. Secondly, the communication is interrupted by occlusions between the LED and camera. Finally, when communicating with multiple LEDs, the proposed method must identify the LED between the two image-sensors. To solve these problem, we will must consider a method which collaborates the images of both cameras in future work.

VII. Conclusion

We proposed a VLC method using PSK. The proposed method uniquely estimates the phase from the pixel values of two cameras with different exposure timings. The feasibility of communication by the proposed method was experimentally validated. We also confirmed that the proposed method can communicate using multi-level PSK. The proposed method is applicable to asynchronous communication, and is potentially applicable to communication with distributed transmitters. In future works, we must improve the Error-Frame detection protocol. Moreover, we will devise a method that collaborates the images of both cameras in the assumed application.

References

[1] M. Akanegawa, Y. Tanaka and M. Nakagawa, "Basic study on traffic information system using LED traffic lights," IEEE Trans. Intelligent Transportation Systems, vol. 2, no. 4, pp. 197-203, Dec. 2001.

[2] T. Komine and M. Nakagawa, "Fundamental analysis for visible-light communication system using LED lights," IEEE Trans. Consumer Electronics,vol. 50, no. 1, pp. 100 107, 2004.

[3] G. Pablo Nava, H. Duy Nguyen, Y. Kamamoto, T. G. Sato, Y. Shiraki, N. Harada and T. Moriya, "A High-Speed Camera-Based Approach to Massive Sound Sensing With Optical Wireless Acoustic Sensors," IEEE Transactions on Computational Imaging, vol. 1, no. 2, pp. 126-139, Jun. 2015.

[4] T. G. Sato, Y. Shiraki and T. Moriya, "Heart Rate Measurement Based on Event Timing Coding Observed by Video Camera," IEICE Transactions on Communications, vol. E100-B, no. 6, pp. 926-931, 2017.

[5] T. Nagura, T. Yamazato, M. Katayama, T. Yendo, T. Fujii, and H.Okada, "Improved decoding methods of visible light communication system for ITS using LED array and high-speed camera," in Proc.IEEE 71st. Vehicular Technology Conf., pp.15, May 2010.

[6] T. Yamazato, I. Takai, H. Okada, T. Fujii, T. Yendo, S. Arai, M. Andoh, T. Harada, K. Yasutomi, K. Kagawa, and S. Kawahito, "Image-sensor-based visible light communication for automotive applications", IEEE Commun. Mag., vol. 52, no. 7, pp. 88-97, Jul. 2014.

[7] T. Yamazato, M. Kinoshita, S. Arai, E. Souke, T. Yendo, T. Fujii, K. Kamakura, and H. Okada, "Vehicle motion and pixel illumination modeling for image sensor based visible light communication", IEEE J. Sel. Areas Commun., vol. 33, no. 9, pp. 1793-1805, Sep. 2015.

[8] C. Danakis, M. Afgani, G. Povey, I. Underwood and H. Haas, "Using a CMOS camera sensor for visible light communication," 2012 IEEE Globecom Workshops, pp. 1244-1248, Dec. 2012.

[9] M. Ohisma, H.Aoyama, K. Nakanishi and T. Maeda, "Image Sensor-based Visible Light Communication Technology," Panasonic Technical Journal, no. 61(2), pp. 118-123, Nov. 2015.

[10] P. Luo, Z. Ghassemlooy, H. Le Minh, X. Tang and H. M. Tsai, "Undersampled phase shift ON-OFF keying for camera communication", 2014 Sixth International Conference on Wireless Communications and Signal Processing (WCSP), pp. 1-6, Oct. 2014.

[11] S. Shimada, N. Akiyama, H. Hashizume and M. Sugimoto, "High-Speed Visible Light Communication with All-purpose Video Camera and Application," IPSJ SIG technical reports, 2016-UBI-50, no. 17, pp. 1-6, May 2016 (in Japanese).

[12] W. Kihara, T. Yendo, S. Arai, T. Yamazato, H. Okada and K. Kamakura, "A Modulation Method to Detect Phase Shift from Asynchronous Camera Image for Visible Light Communication," RISP International Workshop on Nonlinear Circuits, Communications and Signal Processing (NCSP), pp. 133-136, Mar. 2017.